

DEAKIN UNIVERSITY, PIGDONS ROAD, GEELONG VICTORIA 3217, AUSTRALIA

longer axis of the sample was fixed while the lateral deformation was applied to its middle part. The deformation was realized by compression between two synchronized anvils. Fig. 1 shows samples before and after deformation. The samples were rotated by 90° between the consecutive deformations. The detailed procedure, and the system itself, is described by Muszka *et al.* in Ref. [3]. The applied amounts of true strains were 5 and 20 in total (strain of 0.5 per each compression). Deformation was conducted at room and at 500°C temperatures accordingly to schedules given in Table 2. Some samples deformed at room temperature were subsequently annealed at 500°C. This annealing was aimed at producing of high angle grain boundaries (HAGBs) due to recovery and recrystallization processes. It was expected that the post-deformation annealing should have improved the ductility and preserve strength.

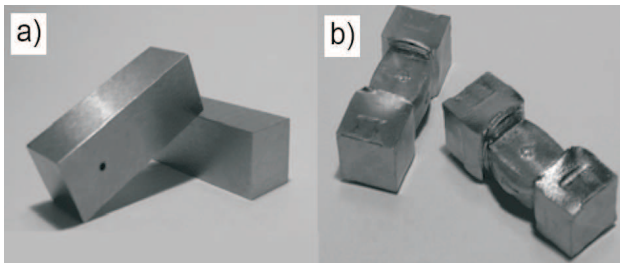


Fig. 1. Macroscopic view of samples before (a) and after (b) deformation on the MaxStrain system

TABLE 2

Treatment routes

No.	ε	Deformation temp., °C	Annealing temp., °C	Annealing time, s
1	5	R.T.	–	–
2	5	R.T.	500	1200
3	20	R.T.	500	1200
4	5	500	–	–

Transmission and scanning electron microscopy (TEM and SEM) were utilized for the microstructural characterization of the samples. Electron Backscattered Diffraction (EBSD) in SEM was used for revealing HAGBs as well as low angle grain boundaries (LAGBs) in a standard manner. Prior to the EBSD, the miniature samples cut out from

the center of the samples (parallel to the fixed axis) were electropolished utilizing a solution of 10% perchloric acid in acetic acid under voltage of 40 V at 10°C. The EBSD measurements were carried out on samples' surfaces with an area of 30×40 μm with step size of 0.15 μm using a LEO 1530 SEM working at a nominal voltage of 20 kV. In the data presented, HAGBs are defined as having misorientations greater than 15° and LAGBs defined as having misorientations of 3–15°. For TEM work, 0.2 mm thick and 3 mm in diameter discs were cut out from a nearby place. The disks were mechanically ground and polished down to 0.05 mm thick foils. Large electron-transparent areas were obtained in these foils by conventional twin jet polishing utilizing the same solution under the same condition as for SEM samples. The foils were examined on a JEOL microscope operated at a nominal voltage of 200 kV.

Tensile tests were carried out at room temperature on flat specimens excised from the central part of the deformed samples along the fixed axis. The gauge dimensions were: length 6 mm, width 3 mm and thickness 2 mm. Due to the small size of tensile specimens the extensometer was not used for the measurement of elongation. The tests were conducted with the frame rate of 2 mm/min on an Instron 4502 testing machine.

3. Results and discussion

Typical TEM microstructures after all processing routes are shown in Fig. 2. The dislocation substructure of the sample 1 was rather “featureless” with a slight tendency toward banded or lamellar type, however, the overall dislocation density was high. The sample 2, annealed at 500°C after true strain of 5, exhibited a more stable configuration of dislocations, however, the overall dislocation substructure was very similar to that one not subjected to the post-deformation annealing. Also, the sample deformed at 500°C (sample 4), i.e. the temperature which is expected to bring about a considerable rearrangement of dislocations due to dynamic recovery, exhibited a dislocation substructure typical for deformation at room temperature rather than at an elevated one.

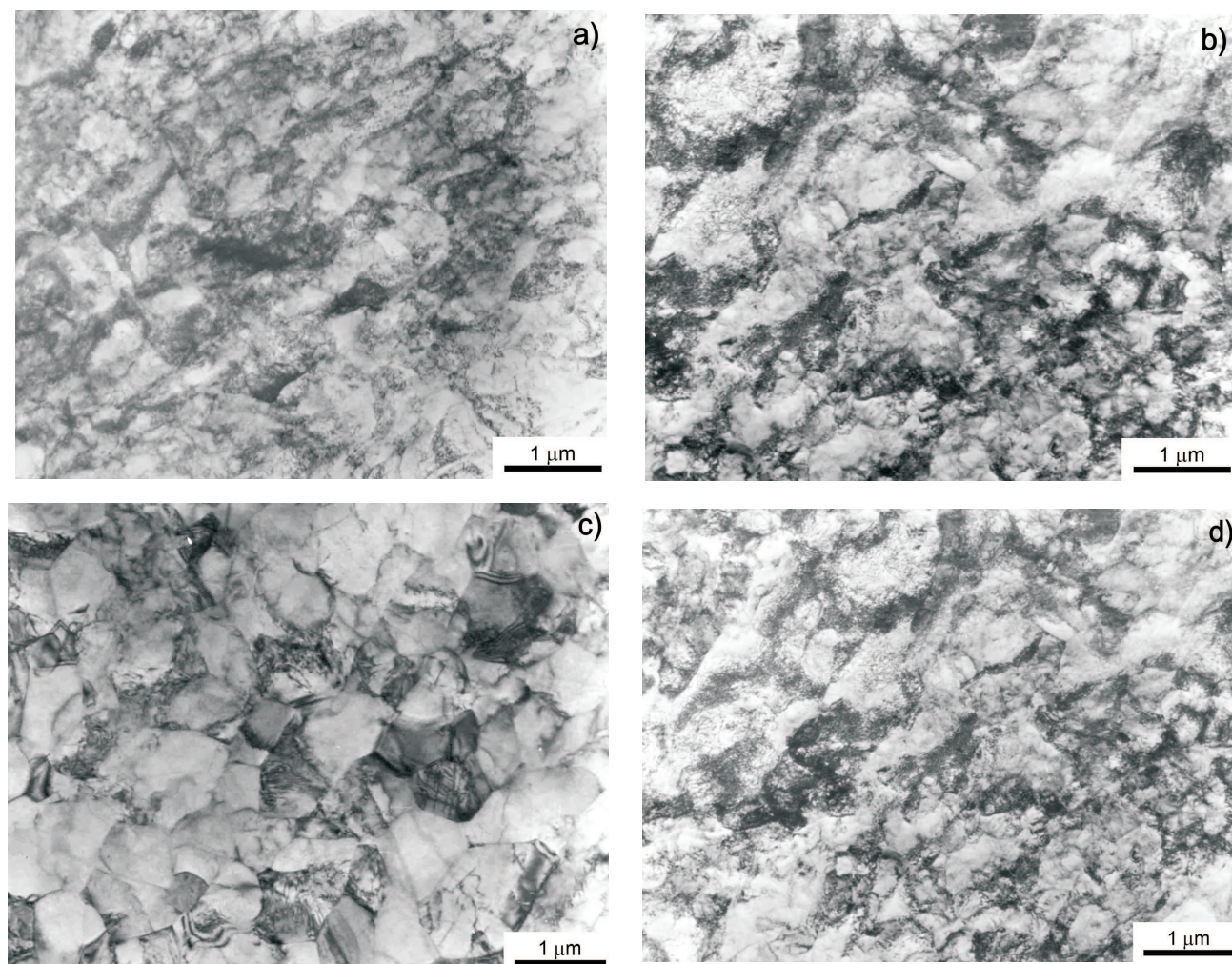


Fig. 2. Typical TEM microstructures of the examined samples: a) route 1; b) route 2; c) route 3; d) route 4

The well defined cells and subgrains, typical for all metals with high stacking fault energy deforming by dislocation glide and subjected to pronounced recovery [4] or continuous dynamic recrystallization (CDRX) [5], were observed after the true strain of 20 followed by annealing at 500°C (sample 3). The dislocation cell substructure evolved toward ultra-fine-grained one as a result of recovery during annealing. However, the TEM micrographs show that the recrystallization was not complete since individual dislocations were still visible in the microstructure (Fig. 2c). The grains and subgrains after this treatment route were equiaxed and their size was estimated as about 0.3-0.5 μm . These values are not precise since a limited area examined by TEM. Usually, majority of the boundaries are of the low-angle dislocation boundary type (misorientations $< 15^\circ$), which is less beneficial for the overall mechanical response. It is difficult for the cells to be transformed into discrete grains surrounded by high-angle grain boundaries without an annealing treatment. The conversion to high-angle misorientation walls usually occurs at a temperature of 0.3-0.4 T_m (melting tem-

perature), which is well below the traditional static recrystallization temperature of 0.5 T_m [6]. The continuous dynamic recrystallization in ferrite is a phenomenon in which misorientation across subboundaries increases continuously with increasing amount of strain until the subboundaries are altered to HAGBs.

In order to more quantitatively evaluate the microstructure of ultrafine grained steels, it has become customary to report not only the average cell or grain sizes and the corresponding grain size distributions, but also the fraction of low- and high-angle grain boundaries obtained from the various processing strategies. Application of EBSD let to reveal the character of the boundaries. Fig. 3 shows exemplary boundary misorientation maps obtained from the EBSD data of the examined steel treated according to routes 2 and 3. The grain boundaries are distinguished in Fig. 3 by different thickness according to the degree of misorientation. The thick lines (black) refer to misorientation angles greater than 15° , i.e. high angle grain boundaries (HAGBs).

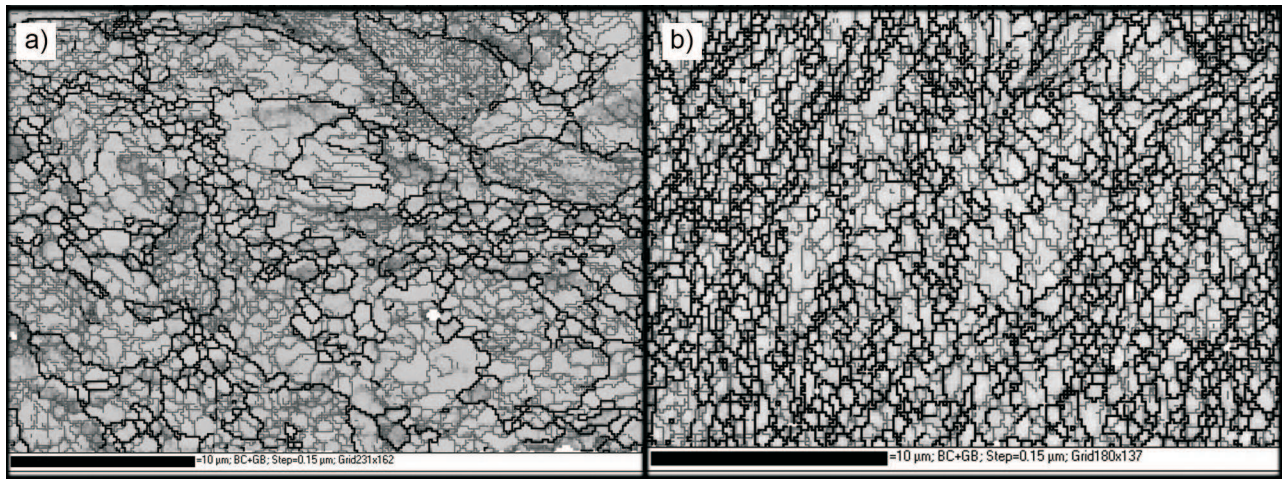


Fig. 3. EBSD maps showing LABs (thin lines) and HABs (thick lines) in samples deformed according to different routes: a) route 2; b) route 3

The thin lines represent low-angle grain boundaries (LAGBs) with misorientations of 3° to 15° . There is a striking difference in the number of the two types of boundaries between particular deformation routes. The microstructures are characterized by the specific distributions of grain boundary misorientations as shown in Fig. 4. The large fraction of LAGBs after true strain of 5 was also observed when the sample was annealed at 500°C . It is a true strain of 20 that changed the predominance of LAGBs into the flat-type misorientation distribution with almost equal fractions of boundaries with different misorientations. The grain size (about $1\ \mu\text{m}$), in this case, was defined as an average distance between HAGBs. The average grain sizes determined by EBSD is larger than the values observed in TEM. This difference, however, is an expected consequence of the fact that both of these techniques utilize different means of identifying grains and grain boundaries [7]. However, in general, the EBSD measurements reproduce the equiaxed structure observed using TEM.

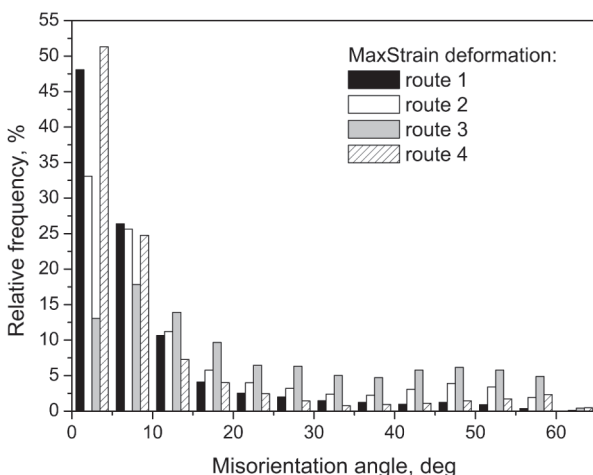


Fig. 4. Distribution of misorientation angles between adjacent ferrite grains/subgrains, at different treatment routes: a) route 1; b) route 2; c) route 3; d) route 4

TABLE 3
Mechanical properties after particular deformation routes

Deformation route	Yield Strength, YS, MPa	Tensile Strength, TS, MPa	YS/TS	Vickers Hardness, HV5
1	470	885	0.53	273
2	598	715	0.84	242
3	504	730	0.69	253
4	326	806	0.40	259

The post-processing annealing have a significant effect on the mechanical properties. The results of tensile and hardness tests are collected in Table 3. The values of hardness in Table 3 pertain to the center of the samples. The tensile test results indicate that the history of the treatment has significant influence on the mechanical properties of the investigated steel. The observed mechanical behavior has been related to the microstructural characteristics of highly strained steel, in which a high density of both dislocations and deformation-induced high-angle boundaries are present. For such structures, mainly dislocation strengthening and grain boundary strengthening contribute to the overall yield strength (YS) and tensile strength (TS) of the material. The post-deformation annealing treatment at 500°C for 0.3 h has brought about an increase in YS and a simultaneous decrease in TS. This mechanical response is not typical for deformed and subsequently annealed metals, where the annealing treatment is expected to lead to the decrease in YS and to the increase in uniform elongation [8]. However, during the tensile test the samples were stretched along the axis perpendicular to the directions of previous deformation what may justify such a behavior. The annealing of sample deformed to the true strain of 20 gave a smaller increase in YS and also smaller decrease in TS and thus improving the possibility

of work-hardening. This happened because of the ferrite grain size decreased and the grain shape became more equiaxed as a result of dynamic recovery. The increase in strength was in accordance with Hall-Petch theory which predicts the yield strength increase by grain refinement. Recovery facilitates the gradual transition of LAGBs into HAGBs.

The effect of the annealing treatment was justified by TEM examination. The investigation revealed a decrease in the dislocation density inside grains. However, single dislocations were still present in the volumes between the boundaries. This observation leads to a suggestion that the observed hardening may be caused by enhanced dislocation recovery due to the interaction between dislocations.

The HAGBs, which are more important for strengthening than LAGBs, are developed especially during deformation to the true strain of 20 and subsequent annealing. Also, HAGBs are more efficient in improving the toughness of steels because when an intragranular cleavage crack moves across a HAGB, the crack front usually branches according to the change of the preferred fracture plane. Such branching results in additional fracture work. In contrast, when a crack meets a low-angle grain boundary, the crack can typically penetrate such an interface without a substantial change in the propagation direction and without branching. That is why, it is necessary to clearly identify and quantitatively characterize the grain boundary character together with the analysis of the grain size [1].

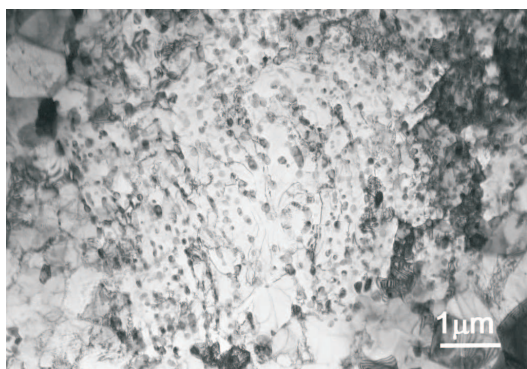


Fig. 5. Globular precipitates of cementite after treatment according to the route 4

Another interesting phenomenon associated with SPD was a morphological change of traditional plate-like pearlite into spheroidized cementite particles (Fig. 5). During plastic deformation pearlitic cementite lamellae disintegrate into short fragments. During large strain deformation and annealing, these fragments spheroidize into discrete cementite particles. The driving force for spheroidization of cementite is the resulting reduction in interfacial area between the cementite lamellae and the ferrite matrix.

4. Conclusions

The mechanisms of microstructure evolution that operated in cold-worked substructures subjected to the annealing at 500°C in C-Mn steel depends significantly on the amount of applied deformation – only the true strain of 20 produces an ultra fine grained structure with a large fraction of high angle grain boundaries. The collective effect of severe deformation and further annealing promotes formation of high-angle grain boundaries and thus stabilizes fine grained microstructure. The refinement of ferrite microstructure results in a significant increase in strength and hardness.

Severe plastic deformation facilitates a transformation of traditional plate-like pearlite into spheroidized cementite particles.

Acknowledgements

The financial support from the AGH University of Science and Technology is greatly appreciated, grant no. 11.11.110.792.

REFERENCES

- [1] R. Song, D. Ponge, D. Raabe, R. Kasper, Microstructure and crystallographic texture of an ultrafine grained C-Mn steel and their evolution during warm deformation and annealing, *Acta Mater.* **53**, 845-858 (2005).
- [2] T. Gladman, *The Physical Metallurgy of Microalloyed Steels*, The Institute of Materials, London (1997).
- [3] K. Muszka, J. Majta, P. Hodgson, Modeling of the mechanical behavior of nanostructured HSLA steels, *ISIJ Int.* **47**, 1221-1227 (2007).
- [4] H.J. McQueen, Elevated temperature deformation at forming rates of 10^{-2} to 10^2 s $^{-1}$, *Metall. Mat. Trans. A* **33**, 345-362 (2002).
- [5] R.D. Doherty, D.A. Hughes, F.J. Humphreys, J.J. Jonas, D. Jul Jensen, M.E. Costner, Current issues in recrystallization, *Mater. Sci. Eng. A* **238**, 219-274 (1997).
- [6] R. Song, D. Ponge, D. Raabe, J.G. Speer, D.K. Matlock, Overview of processing, microstructure and mechanical properties of ultrafine grained bcc steels, *Mater. Sci. Eng. A* **441**, 1-17 (2006).
- [7] T. Neudorf, D. Canadian, H.J. Maier, I. Karaman, The role of heat treatment on the cyclic stress-strain response of ultra fine-grained interstitial-free steel, *Int. J. Fatigue* **30**, 426-436 (2008).
- [8] F.J. Humphreys, M. Hatherly, *Recrystallization and Related Annealing Phenomena*, Pergamon, Oxford (1996).